Journal of Bioelectricity

ISSN: 0730-823X (Print) (Online) Journal homepage: https://www.tandfonline.com/loi/iebm18

# Electromagnetic Modulation of Cell Function: Frequency Characterizations of Input Waveforms

Arthur A. Pilla & Jonathan J. Kaufman

**To cite this article:** Arthur A. Pilla & Jonathan J. Kaufman (1984) Electromagnetic Modulation of Cell Function: Frequency Characterizations of Input Waveforms, Journal of Bioelectricity, 3:1-2, 3-18, DOI: 10.1080/15368378409035955

**To link to this article:** https://doi.org/10.1080/15368378409035955

Published online: 07 Aug 2009.

JOURNAL OF BIOELECTRICITY, 3(1&2), 3-18 (1984)

# ELECTROMAGNETIC MODULATION OF CELL FUNCTION: FREQUENCY CHARACTERIZATIONS OF INPUT WAVEFORMS

Arthur A. Pilla and Jonathan J. Kaufman
Bioelectrochemistry Laboratory
Department of Orthopedic Surgery
Mount Sinai School of Medicine
New York, NY 10029

## ABSTRACT

The requirement that low level electromagnetic modulation of cell and tissue function appears to require specific amplitude and power frequency relationships is examined. Both real and imaginary (Fourier) axis Laplace transformations are employed. A specific frequency range in the various spectra emerges as relevant to obtain biological response. These frequencies appear to correlate with experimentally observed electrochemical relaxation processes at cell membranes.

## INTRODUCTION

Cells and tissues in vitro and in vivo exhibit functional sensitivity to weak pulsating currents. Reactively coupled (external to laboratory dish or skin) signals have been employed in a variety of cell and tissue types (1-19,35). Emerging from all of these studies is the existence of both electrical and biological windows (2-4,7,8, 11,12,17,18,20). Thus, while significantly different waveforms have been successfully employed, it appears that certain frequency domain characteristics of the signals are necessary. It is the purpose of this work to examine the use of various forms of Laplace transformation using both the real axis (21,22) and imaginary axis (Fourier analyses) to quantitate signal differences.



 0730-823X/84/0301-0003$3.50/0

## FREQUENCY DOMAIN SIGNAL ANALYSIS

For the variety of time varying signals which have been employed for cell and tissue stimulation it is convenient to describe the waveform parameters in terms of the amplitude or power variations over a given frequency range. This may be accomplished by the use of the Laplace transformation in its most general sense. For an arbitrary time function, f(t), the Laplace transform, F(s), is given by:

$$F(s) = \int_0^\infty f(t)e^{-st}\,dt \qquad (1)$$

where s defines the complex frequency plane having real, $\sigma$, and imaginary, $j\omega$, axes. For $s = \sigma$ the real axis transformation is defined, the frequency functions obtained are real and have been found useful for cell impedance studies as well as signal description (23-27). For $s = j\omega$ the operation is the familiar Fourier transform (or series) and is most useful for the description of the amplitude or power spectrum of the input signal and system response.

In order to illustrate the use of this approach, inductively coupled, approximately rectangular shaped electric field signals will be considered. These have been most extensively employed in the modulation of cell and tissue function. Generally the induced electric field is bipolar in nature. Amplitude and time assymetry are controlled. Pulse durations from 20 μsec to 6 msec having repetition rates from 1-100 Hz are common. For the major clinical application to recalcitrant bone fractures (28-31) a pulse burst signal has been employed. Waveform types considered in this study are shown in fig. 1. The use of equation (1) in this study will be limited to consideration of the input (electric field) signal. It

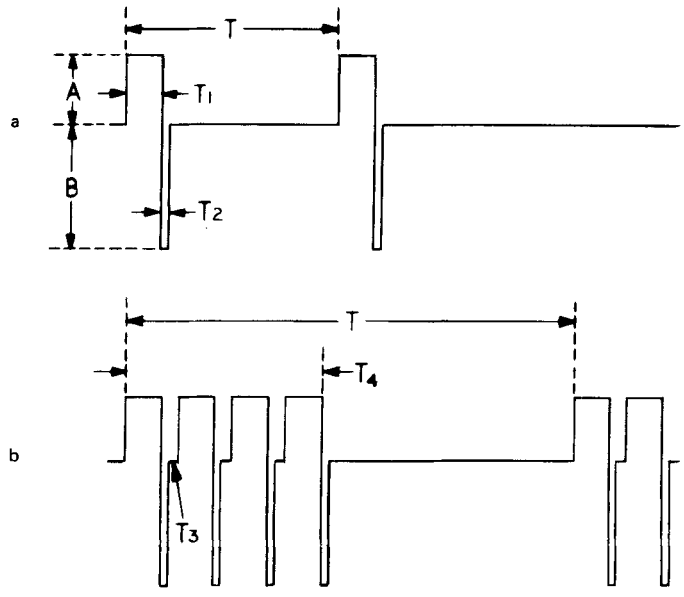


FIGURE 1

Schematic illustration of the input voltage (at the cell) for two widely employed, inductively coupled waveforms. Signal b is the pulse burst employed clinically for recalcitrant bone fracture repair when T1 = 200 μsec, T2 = 20 μsec, T3 = 8 μsec, T4 = 5 msec and T = 67 msec (15 Hz).

has, however, been suggested that a model dependent frequency analysis, using the hypothesis that electrochemical kinetics at the cell surface are the real-time current pathways, would be most useful. This will be considered elsewhere.

## A - REAL AXIS LAPLACE TRANSFORMATION

This is performed for $s = \sigma$ and can be utilized to obtain the frequency spectrum of the input voltage and the input power (resistive load). For the former the transform becomes, for a single repetitive bipolar pulse (a, fig. 1):

$$V(\sigma) = \frac{A}{\sigma(1-e^{-T\sigma})}\left[1-e^{-\sigma T1} - \frac{T1}{T2}\, e^{-\sigma T1}\,(1-e^{-\sigma T2})\right] \qquad (2)$$

where T1, T2 and T are the main and opposite polarity pulse widths and the pulse period respectively. This spectrum is illustrated in fig. 2. While an accurate indication of the input voltage frequency spectrum, it is not sensitive to signal variations which have been shown to move the waveform parameters out of the effective window for observed cellular effect. Thus fig. 2 shows the effect of a 4 fold variation in T2 - from 20 μsec (effective) to 5 μsec (ineffective). The differences are too small to be considered meaningful for a sensitive signal description. This is in marked contrast to

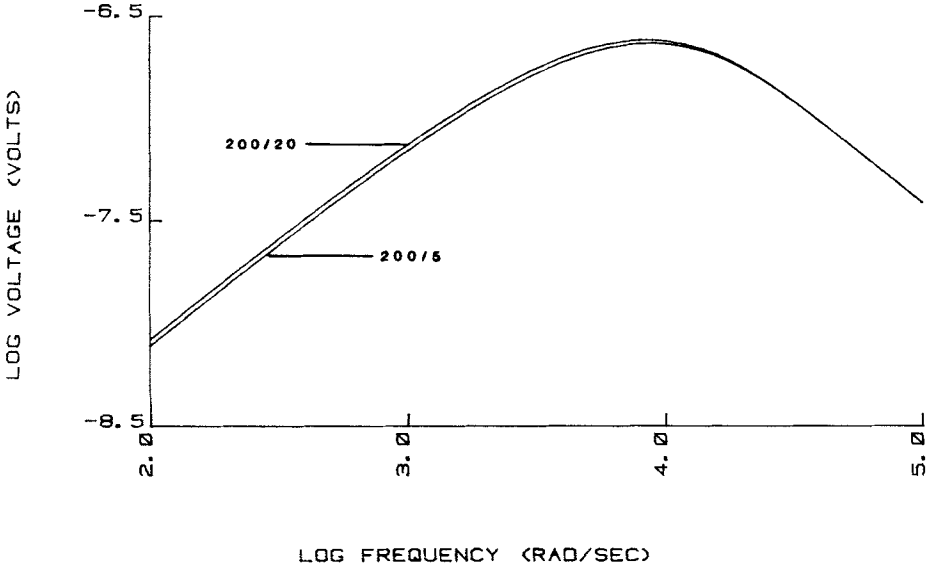


FIGURE 2

Real axis spectrum of the voltage (a, fig. 1) for T2 = 20 μsec (upper curve) and T2 = 5 μsec (lower curve) obtained via equation (2). For both spectra T1 = 200 μsec and T = 67 msec. Note the lack of sensitivity for variations in T2.

the standard amplitude spectrum (via s = jω) as will be seen below.

The spectrum of the input power, P(σ), is given by:

$$P(\sigma) = \frac{A^2}{\sigma(1-e^{-T\sigma})} \left[1-e^{-\sigma T1} - \frac{T1^2}{T2^2} e^{-\sigma T1} (1-e^{-\sigma T2})\right] \qquad (3)$$

where the symbols are as for equation (2). In contrast to V(σ), a plot of P(σ) for the same 4 fold variation in T2 as above, shows a large difference in the medium to high frequency range (fig. 3). This spectrum emphasizes, as expected, the large changes in instantaneous power which occur due to the constraint of identical areas (32) under the 20 μsec and 5 μsec signals.

It is of interest to consider the spectrum of the power, P'(σ), for the pulse burst signal commonly employed in cell stimulation studies (b, fig. 1). This is given by:

$$P'(\sigma) = P(\sigma) \left[\frac{1-e^{-(M+1)\sigma TA}}{1-e^{-\sigma TA}}\right] \qquad (4)$$

where M+1 is the number of pulses in the burst and TA is T1 + T2 + T3 (see b, fig. 1). This is also shown in fig. 3, wherein it can be seen that the spectrum of the power in the higher frequency range is significantly larger for the single pulse having 5 μsec opposite polarity (T2) than that for the pulse burst. This has implications in the choice of the most efficient signal coupling to real-time cell surface kinetics as will be seen below.

## B - IMAGINARY AXIS LAPLACE TRANSFORMATION

This actually constitutes the well known Fourier analysis and

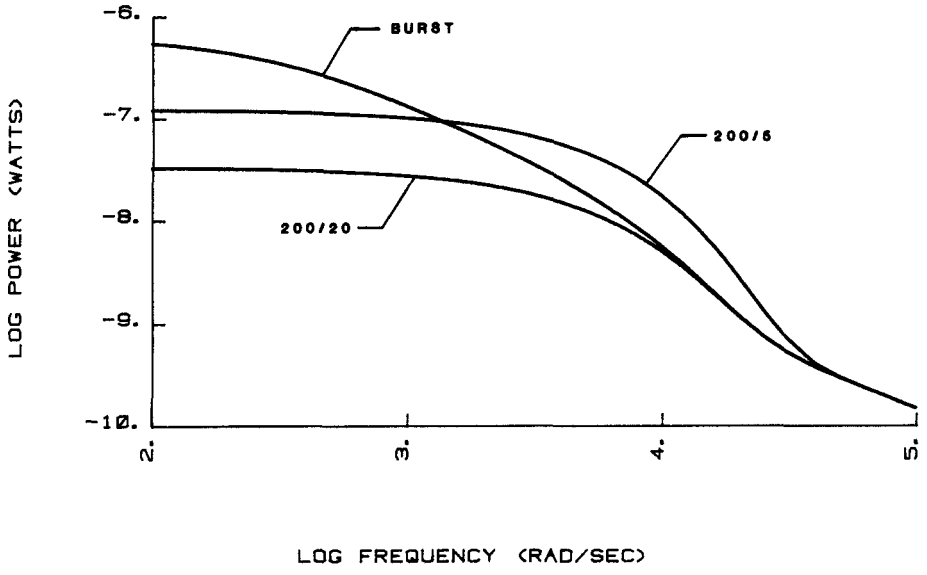


FIGURE 3

Real axis spectrum of the power for both signals considered in fig. 2, as well as the pulse burst signal (b, fig. 1) obtained via equation (3). Note the mid to high-frequency range over which the 200/20 single pulse and the pulse burst have identical spectra. In contrast the 200/5 single pulse exhibits significantly higher values over (particularly) the mid-frequency range.

is represented by equation (1) evaluated for $s = j\omega$. The Fourier transform of a periodic signal is represented by a sequence of delta functions existing at the harmonics of the signal, v(t), with strengths equal to the coefficients of the Fourier series (33). Thus:

$$v(t) = \sum_{n=-\infty}^{\infty} V_n \, e^{jn\omega_o t} \quad . \tag{5}$$

The (complex) Fourier coefficients $V_n$ are obtained via:

$$V_n = \frac{1}{T} \int_{-T/2}^{T/2} v(t) e^{-jn\omega_o t} \, dt \quad , \tag{6}$$

with $\omega_o = \frac{2\pi}{T}$ being the fundamental frequency associated with the signal v(t) and T its period. The information contained in the set $\{V_n, n = 0,\pm1,\pm2, \ldots\}$ is equivalent to that in the original signal. Thus, since $V_n$ is complex, it may be written as:

$$V_n = |V_n| \, e^{j\theta_n} \quad . \tag{7}$$

The real amplitude $|V_n|$ and the phases $\theta_n$ completely specify the signal v(t) and may each be plotted as a function of n. Only the amplitude sepctrum $|V_n|$ will be considered here. The more complex phase spectrum, $\theta_n$, will be considered elsewhere. The average power of the signal v(t) as given by:

$$P_{av} = \frac{1}{T} \int_{o}^{T} v^2(t) \, dt \tag{8}$$

can also be expressed in the frequency domain as:

$$P_{av} = \sum_{k=-\infty}^{\infty} |V_k|^2 = \sum_{k=1}^{\infty} 2 |V_k|^2 \tag{9}$$

Thus, a plot of the amplitude spectrum $|V_k|$ or power spectrum $|V_k|^2$ is proportional to the power in the signal v(t) in a particular region of the spectrum.

The signals to be analyzed here are shown in fig. 1. The Fourier series coefficients $V_k$ may most simply be derived by first considering the single repetitive pulse p(t) (a, fig. 1). Denoting

the Fourier coefficients of p(t) by $P_k$, and defining $TA \triangleq T1 + T2 + T3$, then $V_k$ for the pulse burst signal (b, fig. 1) may be expressed as:

$$V_k = P_k \left[ 1+e^{-jk\omega_o TA} + \ldots + e^{-jk\omega_o MTA} \right] \tag{10}$$

$$\text{or} \quad V_k = P_k \sum_{\ell=0}^{M} e^{-jk\ell\omega_o TA} \quad ,$$

where M+1 is equal to the total number of bipolar pulses in one period of v(t). Expressing the summation in (11) in closed form through use of the finite sum geometric formula, the amplitude spectrum of v(t) is:

$$|V_k| = |P_k| \, |B_k| \quad , \tag{12}$$

where

$$|B_k| = \left| \frac{\sin[k\omega_o TA(M+1)/2]}{\sin[k\omega_o TA/2]} \right| \quad . \tag{13}$$

Thus, $|V_k|$ can be decomposed into the product of the single repetitive pulse spectrum $|P_k|$ and the "burst" spectrum $|B_k|$. Note that for single pulse trains (M=0), $|B_k| = 1$ as required. This decomposition leads to some useful insights in the analysis of stimulation signals as discussed below.

The Fourier amplitude coefficients $|P_k|$ are obtained through straightforward application of (6) and are given by:

$$|P_k| = \frac{1}{T} \left[ \sigma_k^2 + \beta_k^2 + 2\,\sigma_k\beta_k \cos\left[k\omega_o \frac{(T1+T2)}{2}\right] \right]^{\frac{1}{2}} \tag{14a}$$

$$\text{with} \quad \sigma_k = AT1 \; \frac{\sin(k\omega_o T1/2)}{(k\omega_o T1/2)} \tag{14b}$$

$$\text{and} \quad \beta_k = BT2 \; \frac{\sin(k\omega_o T2/2)}{(k\omega_o T2/2)} \tag{14c}$$

Equations (12)-(14) completely characterize the signal amplitude spectrum. Several features of this spectrum are important and should be pointed out:

(i) The burst spectrum $|B_k|$ acts as a multi-bandpass filter as can be seen by looking at fig. 4. The

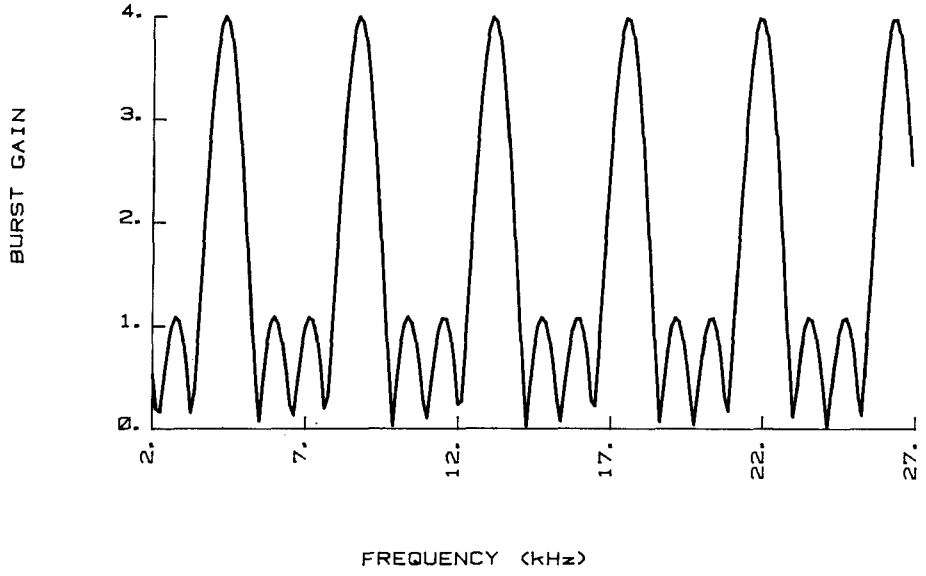


FIGURE 4

Imaginary axis (Fourier) amplitude spectrum of the burst portion of the clinical signal (b, fig. 1) obtained via equation (13). Note that the "spikes" appear at harmonics of the pulse period within the burst (T1 + T2 + T3 = 228 μsec, corresponding to 4.4 kHz). This acts as a gain function for the single repetitive pulse (from which the burst is constructed) in the frequency domain.

resonant frequencies are determined by TA and for the example shown (TA = 228 msec) resonance occurs at integral multiples of $f_o$ = 4.4 kHz.

(ii) For the typical case of signal parameters where T1 $\geq$ 10T2 and AT1 = BT2 (see fig. 1), $|P_k|$ behaves as a uni-polar pulse spectrum, i.e., sinx/x, at least above the very lowest frequencies.

(iii) The effect of repetition rate (1/T) on the overall pulse spectrum is indistinguishable from a change in amplitude (squared). Thus, as far as (linear) system response is concerned, it is possible to keep T fixed and vary only signal amplitude A, which simplifies the analysis.

Several different pulse spectra are presented in figs. 5 and 6 following equations (12)-(14). Figure 5 displays the amplitude spectrum of the same pulse burst signal for which the corresponding real axis spectrum of the power is shown in fig. 3. The spiked nature of the spectrum is due to the repetition rate within the "burst" portion (4.4 kHz for the clinical signal). The spectra of three signals, similar to those described in fig. 3 for real axis transformation are shown in fig. 6. The spectrum marked 200/20 is that for a single pulse from which the burst signal is constructed (for the clinical signal there are 21 such pulses in a given burst) having the same repetition rate as the burst (15 Hz). Note that there are no "spikes" in this spectrum, but that the amplitude follows closely that of the burst between "spikes". As for the real axis, the spectrum of the signal having T2 = 5 μsec (marked 200/5 in fig. 6) shows that it has significantly higher amplitude

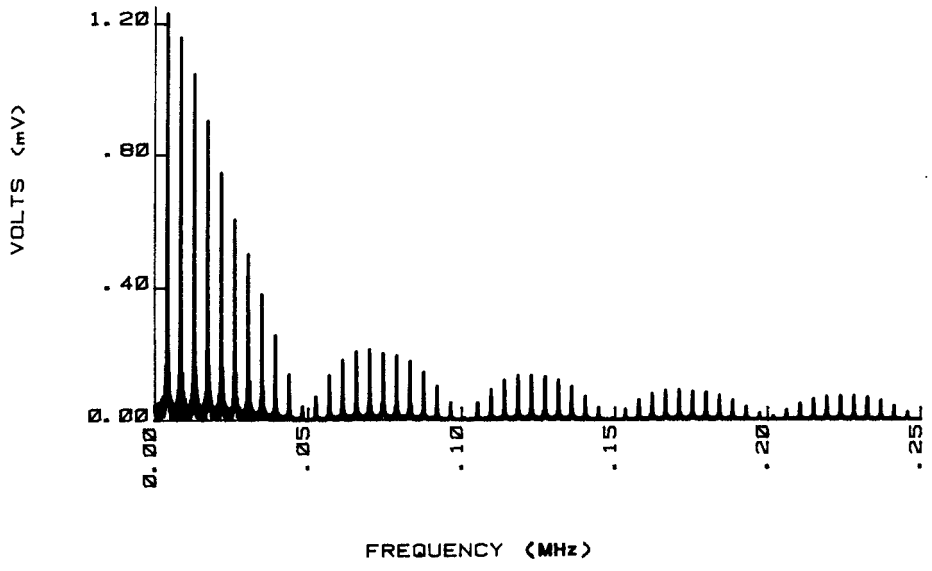


FIGURE 5

The complete Fourier spectrum of the pulse burst inductively coupled signal used clinically. T1 = 200 μsec, T2 = 20 μsec, T3 = 8 μsec, T4 = 5 msec, T = 67 msec (15 Hz).

in the higher frequency range than that for the 200/20 or the inter "spike" regions of the burst.

## DISCUSSION

The use of both real and imaginary axis Laplace transformations to describe various amplitude and power relationships in the frequency domain is useful to examine the frequency range over which amplitude must be maintained to elicit biological effect. For example, several systems have exhibited similar response to both the pulse burst and a single repetitive pulse from which the burst portion is constructed (25). Examination of fig. 6 shows that, over the mid-frequency range depicted, both the single pulse and

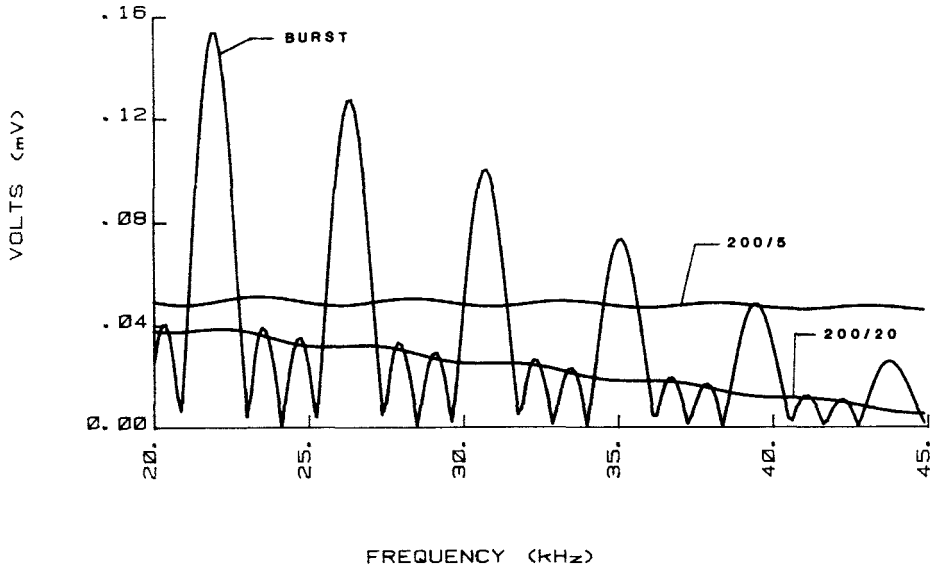


FIGURE 6

Comparison of the Fourier amplitude spectra for the signals considered in fig. 3. Note that the inter spike amplitude for the pulse burst and 200/20 single repetitive pulse (both at 15 Hz) are nearly identical. In contrast, the 200/5 single pulse (15 Hz) exhibits significantly higher amplitude over the indicated frequency range (compare with fig. 3).

inter-spike regions of the pulse burst exhibit similar amplitudes. This is also true of the real axis spectrum of the power for both signals, as shown in fig. 3. One possible interpretation is that the biological system ignores the much greater amplitudes present at the burst harmonics and responds only at amplitude levels corresponding to the inter-burst frequencies. This is reinforced by consideration of the spectra for the single pulse having T2 = 5 μsec (figs. 3 and 6). Here, for a signal having no burst spikes, the amplitude is higher over the depicted range for all frequencies except those corresponding to the intra-burst repetition rate of

the pulse burst signal. Remarkably, several biological systems exhibit no response (26,28,34) or greatly altered response (15) to signals for which the opposite polarity amplitude (b, fig. 1) is significantly increased by a decrease in T2 (i.e., the 200/20 vs. the 200/5 signals discussed in this study). Note that the effect on a burst signal, for which only T2 is decreased, is exactly similar to the single pulse cases.

The above correlations lead to the proposal that the amplitudes of importance to the biological system are those generated in the spectra of the opposite polarity (T2) portion of both single and burst pulses considered here. In addition, values in the mid to high frequency range (> 20 kHz) appear to be the most relevant. Results from impedance studies of living cell membranes (23,24,27) show the existence of a heterogeneous potential dependent kinetic process having a relaxation time in the range of 10-100 μsec. This process, which exhibits the functionality of specific adsorption (ion binding), easily falls within the frequency range of interest. If, as suspected, perturbation of these electrochemical pathways are of functional significance to the cell, then it is obvious that any signal, which exhibits similar amplitudes or powers in specific frequency ranges corresponding to those for which the electrochemical kinetic filter at the cell surface is open, can be effective.

Clearly, the analysis presented here can be applied to any waveform, including sine, from any source which can achieve the required amplitude and/or power relationships in the frequency domain. It is also clear that the discovery of an effective range is merely the first step in the choice of the most effective

signal for the modulation of cell and tissue function. Aspects, such as time dose requirements are not able to be easily predicted by this analysis alone. A frequent observation, however, is that the proper signal parameters must be chosen before dose analyses can be effective. Finally, it is important to emphasize that the required amplitude/power relationships must be achieved at the appropriate cell(s). Thus, geometric considerations, and their effects on the overall impedance of the system, must be taken into account (32) particularly when inductively coupled signals are employed. The analyses presented here are general enough to characterize the input waveform at the cellular level considering all of the above points. These frequency characterizations are the first step in establishing a standard by which dose relationships versus cell type and pathology may be quantitated.

## REFERENCES

( 1) Adey, W.R.: Proceedings IEEE 68, 119, 1980.

( 2) Assailly, J.; Monet, J.-D.; Goureau, Y.; Christel, P. and Pilla, A.A.: Bioelectrochem. Bioenergetics 8, 515, 1981.

( 3) Bassett, C.A.L.; Pawluk, R.J. and Pilla, A.A.: Ann, N.Y. Acad. Sci. 238, 242, 1974.

( 4) Bawin, S.M ; Adey, W.R. and Sabbot, I.J.: Proc. Nat. Acad. Sci., U.S.A. 75, 6314, 1978.

( 5) Blackmann, C.F.; Benane, S.G.; Joines, W.T.; Hollis, M.A. and House, D.E.: Bioelectromagnetics 1, 277, 1980

( 6) Cheng, N.; van Hoof, H.; Bockz, E.; Hoogmertens, M.J.; Mulier, J.C.; DeDijker, F.J.; Sansen, W.M. and DeLoecker, W.: Clin. Orthoped. 171, 264, 1982.

( 7) Chiabrera, A.; Hinsenkamp, M.; Pilla, A.A.; Ryaby, J.; Ponta, D. and Nicolini, C.: J. Histochem. Cytochem. 27, 375, 1979.

( 8) Christel, P.; Cerf, G. and Pilla, A.A.: In "Mechanisms of Growth Control," R.O. Becker, ed., Charles C. Thomas, Springfield, 237, 1981.

( 9) Colacicco, G. and Pilla, A.A.: Bioelectrochem. Bioenergetics 10, 119, 1983.

(10) Dixey, R. and Rein, G.: Nature 296, 253, 1982.

(11) Goodman, R.; Bassett, C.A.L. and Henderson, A.S.: Science 220, 1283, 1983.

(12) Luben, R.A.; Cain, C.D.; Chen, M.C.-Y.; Rosen, D.M. and Adey, W.R.: Proc. Nat. Acad. Sci. U.S.A. 79, 4180, 1982.

(13) Norton, L.: Clin. Orthoped. 167, 280, 1982.

(14) Rodan, G.A.; Bourrett, L.A. and Norton, L.A.: Science 199, 690, 1978.

(15) Smith, S.D. and Pilla, A.A.: In "Mechanisms of Growth Control," R.O. Becker, ed., Charles C. Thomas, Springfield, 137, 1981.

(16) Ubeda, A.; Leal, J.; Trillo, M.A.; Jimenez, M.A. and Delgado, J.M.R.: J. Anat. 137, 513, 1983.

(17) Smith-Sonneborn, J. and Pilla, A.A.: J. Electrochem. Soc. 129, 132C, 1982.

(18) Sisken, B.F.; Fowler, I. and Pilla, A.A.: J. Electrochem. Soc. 126, 143C, 1979.

(19) Brighton, C.T.; Cronkey, J.E. and Osterman, A.L.: J. Bone Joint Surg. 58A, 971, 1976.

(20) Pilla, A.A.: Ann. N.Y. Acad. Sci. 238, 149, 1974.

(21) Pilla, A.A.: J. Electrochem. Soc. 117, 467, 1970.

(22) Pilla, A.A.: In "Electrochemistry, Calculations, Simulation and Instrumentation," J.S. Mattson, H.B. Mark, Jr. and H.C. McDonald, Jr., eds., Marcel-Dekker, New York, 110-142, 1973.

(23) Pilla, A.A. and Margules, G.S.: J. Electrochem. Soc. 124, 1697, 1977.

(24) Schmukler, R. and Pilla, A.A.: J. Electrochem. Soc. 129, 526, 1982.

(25) Pilla, A.A.: In "Bioelectrochemisty," H. Keyzer and F. Gutmann, eds., Plenum Press, New York, 353, 1980.

(26) Pilla, A.A.: In "Mechanisms of Growth Control," R.O. Becker, ed., Charles C. Thomas, Springfield, 211, 1981.

(27) Margules, G.S.; Doty, S.B. and Pilla, A.A.: Adv. Chem. Series 188, 108, 1980.

(28) Bassett, C.A.L.; Pilla, A.A. and Pawluk, R.J.: Clin. Orthoped. 124, 117, 1977.

(29) Bassett, C.A.L.; Mitchell, S.N. and Gaston, S.R.: J. Bone Joint Surg. 63A, 511, 1981.

(30) Bassett, C.A.L.; Mitchell, S.N. and Schink, M.M.: J. Bone Joint Surg. 64A, 1214, 1982.

(31) Sedel, L.; Christel, P.; Duriez, J.; Duriez, R.; Evrard, J.; Ficat, C.; Cauchoix, J. and Witovet, J.: Rev. Chir. Orthoped. 67, 11, 1981.

(32) Pilla, A.A.; Sechaud, P. and McLeod, B.R.: J. Biol. Phys. 11, 51, 1983.

(33) Schwarz, R.J. and Friedland, B.: In "Linear Systems," McGraw-Hill, New York, 136-143, 1965.

(34) Hellman, K. and Pilla, A.A.: Unpublished results.

(35) Norton, L; Pilla, A.A.; Regelson, W. and Tansman, L.: J. Electrochem. Soc. 127, 130C, 1980.